Carbon dioxide sorption and melting behaviour of mPEG-alkyne.

S. López, M.J. Ramos, J.M. García-Vargas, M. T. García, J.F. Rodríguez, I. Gracia*.

Institute of Chemical and Environmental Technology (ITQUIMA), Department of Chemical Engineering, University of Castilla-La Mancha, Avda. Camilo José Cela 1A, 13005 Ciudad Real, Spain.

*Corresponding author: Ignacio.Gracia@uclm.es

Telf:+34926 29 53 00 ext. 3419

Abstract

The understanding of the phase behaviour of the mixture mPEG-alkyne and supercritical CO_2 ($scCO_2$) and the study of the variation of the polymer melting point are essential prerequisites in order to determine appropriate operating conditions and develop high pressure processes that allow the obtention of a conjugate mPEG-alkyne with a drug or a protein. In this work, it was observed a progressive decrease of the melting point temperature of mPEG-alkyne induced by the adsorption of CO_2. The obtained melting temperatures were correlated using a modification of the Clausius Clapeyron equation. The equilibrium sorption of CO_2 into mPEG-alkyne was determined with a variable-volume view cell employing a static method. These experiments were carried out in the temperature range 308 and 318 K, and at 8-17 MPa of pressure. The predictability of the models of Henry's Law, Dual-Mode, Sanchez Lacombe Equation of State and Heuristic Model was evaluated.

Keywords

Supercritical CO_2, mPEG-alkyne, melting point, sorption.

1. Introduction

Polyethylene glycol (PEG) is a polyether composed of repeated ethylene glycol units [-$(CH_2CH_2O)_n$]. PEGs have an indispensable role as packaging in drug delivery systems (DDS) in pharmaceuticals, because of its high structure flexibility, biocompatibility, amphiphilicity, hydration capacity and devoid of any steric hindrances [1]. It is the most commonly used protective coating material for drug delivery liposomes, nanoparticles, and has also provided the same protection as a covalently bound conjugate to proteins and other drug molecules [2]. It can also be presented in different states, as PEG samples with low relative molecular weight (MW: 100-700) are liquids at room temperature, while at relative molecular weight between 1000 and 2000 are soft solids, and PEGs with MW >2000 are hard crystalline solids with melting points of around 63 ºC. PEG also exhibits a low glass transition temperature (from (-70 to -10) ºC depending on its molecular weight), which imparts a rubbery characteristic to the material, what results in high permeability [3]. Covalent conjugates of PEG and drugs or proteins have already been commercialized successfully [4,5]. Due to the presence of only two functional groups in PEG, what limits the scope for further derivatization with targeting ligands, commercial methoxy-poly(ethyleneglycol) alkyne (mPEG-alkyne) was used in this study [3], [6]. One of the approaches widely used recently in the conjugation of drug-polymer involves “click chemistry”. Click chemistry promotes the use of organic reactions that allow the connection of two molecular building blocks in a facile, selective, high-yield reaction under mild conditions with few or no by-products. One of the most interesting click reactions is the Copper(I)-catalyzed alkyne-azide cycloaddition (CuAAC), which implies the reaction between azide and terminal alkynes. Click chemistry is usually carried out using organic solvents such as THF or DMF [7–9]. In order to avoid

52 the use of organic solvents that involves the presence of harmful residues in pharmaceutical
53 presentatiosn following the statements of green chemistry, extensive effort has been focused
54 on the use of cleaner methods for the processing of polymers [10].

55 One of such methods is the use of supercritical CO_2 as reaction media and/or processing
56 solvent. In the last years supercritical carbon dioxide ($scCO_2$) has been widely used in
57 polymer processing technologies such as polymerization, polymer functionalization,
58 foaming, impregnation and encapsulation. In addition, the use of $scCO_2$ has attracted interest
59 in the production of biodegradable/biocompatible polymers for pharmaceutical and medical
60 applications [11–13].

61 Some polymers can absorb significant amount of CO_2 as a result of the ability of this gas to
62 weakly interact with basic sites along the macromolecular chains [14,15]. The CO_2 is diffused
63 between the polymer chains and its sorption increases the free volume and mobility of the
64 polymer segment. The CO_2 acts as lubricant making easier the friction between the polymer
65 chains and softening of the polymer, allowing polymers to become viscous liquids without
66 the need of organic solvents and elevated temperatures [16]. In the case of semi-crystalline
67 polymers, the plasticization or swelling effects are even stronger since the dissolution of CO_2
68 increases the mobility of the chain. This mobility is owed to the plasticizing effect of CO_2,
69 which induces recrystallization with altered kinetics and/or rearrangement of crystalline
70 morphologies [17–20]. Sorption of supercritical fluid in a polymer can lower its melting
71 temperature (T_m), significantly below that seen at atmospheric pressure. For a given polymer,
72 the melting temperature depression is found to increase as the amount of $scCO_2$ sorbed
73 increases. Therefore, it is very important to understand the influence of CO_2 at different
74 pressure on the melting point of the mPEG-alkyne and the phase equilibrium data of the

system [21–23]. Regarding this topic, a review has been published by Knez et al. [20] in which two methods to determined T_m of PEG are described and compared. These methods are a capillary method in a high pressure optical cell and High-Pressure Differential Scanning Calorimetry (HP DSC) [20]. HP DSC is a powerful tool which allows to study in-situ the thermal transition in presence of CO_2 or other gases at high pressure. It gives the opportunity to understand the interaction of polymer and gas molecule in situ and its most important advantage is that the systematic error done by researcher could be minimized.

In this respect, some authors investigated PEG/CO_2 system under different temperatures and pressures, which offer useful information with the purpose of determine requisite processing conditions. Nowadays, various methods for the solubility measurements at elevated temperatures and pressures have been published to measure the sorption of CO_2 into PEG [24]. The best known methods are gravimetric [25,26] chromatographic [27], spectroscopy [28] and the phase separation method [17,29–32], which is the most commonly used.

The combination of polymer and $scCO_2$ has made it possible to obtain successful drug polymeric carriers in several presentations, scaffolds, microparticles, microcapsules, etc. In order to design an empirical method to develop chemical reactions or processing operations with $scCO_2$, it is essential to study the phase behaviour between $scCO_2$ and the main substances playing a role in the desired process. To perform the click chemistry functionalization of PEG based polymer with a molecule of interest, it is necessary to have a PEG in its alkinated or azidated form. This change of its molecular structure will also involve small or large variations in its interaction with the $scCO_2$. To the best of our knowledge the equilibria between mPEG-alkyne and scCO2 has not been reported yet in literature.

97 In the present work, melting temperature and experimental sorption of $scCO_2$ into a mPEG-
98 alkyne and a modelling study will be reported. The study of these properties was carried out
99 for a mPEG 2000 $g \cdot mol^{-1}$ because it is widely used as a gold standard in bioconjugation and
100 nanomedicine to prolong blood circulation time and improve drug efficacy [33–35]. The
101 sorption has been determined with a gravimetric method using an external balance and we
102 compare the obtained experimental results with different studies. Thermodynamics
103 modelling is a common approach to the study of the phase equilibrium. Several methods to
104 modelling $scCO_2$-polymer systems are available in literature, and in this work, Sanchez-
105 Lacombe equation of state (SL EOS) and the heuristic model were selected in order to
106 correlate the phase equilibrium of the working system due to their greater mathematical
107 simplicity and proper fit [36–38].

108

109 # 2. Experimental

110

111 ## 2.1. Materials

112 Methoxy polyethylene glycol alkyne (mPEG-alkyne) 2000 $g \cdot mol^{-1}$ was obtained from
113 creative PEGWorks (North Carolina) and was used without further purification. Carbon
114 dioxide (CO_2) with a purity of 99.8% was obtained from Carburos Metálicos S.A. (Spain)
115 without further purification.

116

2.2. Equipment and methods

2.2.1. High Pressure Differential Scanning Calorimetry (HP DSC)

The sorption of CO_2 induced depression of the melting temperature of mPEG-alkyne. This depression was determined by using High Pressure Differential Scanning Calorimetry (HP DSC) as a function of temperature and/or pressure. A schematic diagram of the experimental setup is shown in Figure 1.

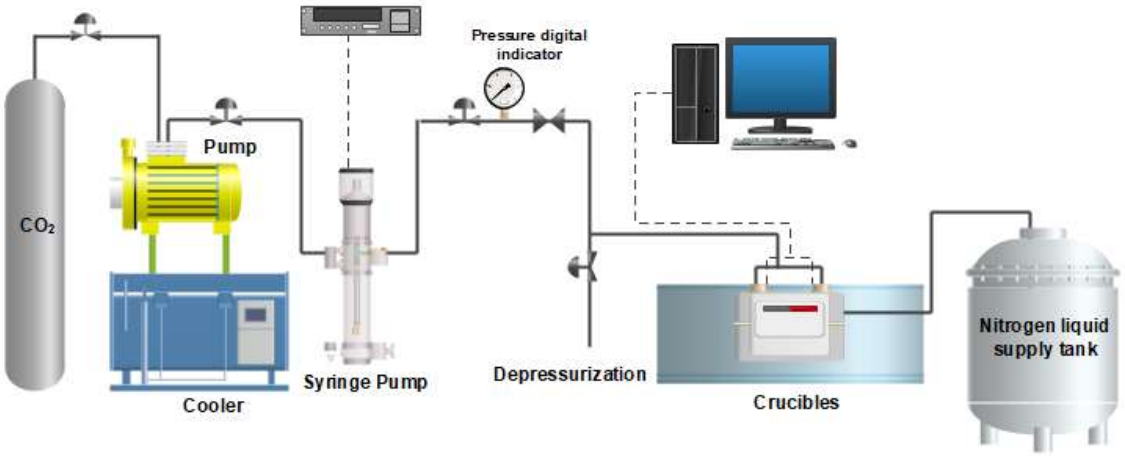

Figure 1.

The experiments were performed in a SENSYS evo DSC (Setaram, Madrid) equipped with two high pressure Inconel crucibles enabling measurements up to 40 MPa. The samples of mPEG-alkyne are placed in the crucibles, weighted and filled with CO_2. CO_2 is cooled and pressurized to the desired value by means of a positive-displacement pump and a syringe pump, which controls the amount of gas fed.

The samples are annealed at the desired pressure for 300 minutes to ensure total CO_2 sorption. For determination of melting temperature T_m the samples were heated at a rate of 10 K/min

from 0 to 150 ºC, cooled at the same rate to 0ºC and reheated to 150ºC. The samples were kept at 0 and 150 ºC for 10 minutes. The melting temperature of the polymer has been determined from the thermogram obtained in the second heating, since the first heating is used to thermally erase the polymer.

After 300 min the samples showed a stable composition, indicating phase equilibrium. When the equilibrium is reached (at least 300 min) the crucible is vented quickly, and the volume of CO_2 is measured through a turbine flowmeter.

- **Clapeyron Equation**

The Clausius-Clapeyron equation can be used to explain the relationship between equilibrium transition temperature and pressure during the phase transition of any subtance. Based on the fact that CO_2 exhibits a poor solvent capacity for most polymers, the polymer fraction in vapor phase is usually negligibly small, and the polymer phase may also be reasonably considered as pure polymer. With these assumptions, the Clapeyron equation could be sum as:

$$\frac{dT_m}{dP} = T\frac{\Delta V_m}{\Delta H_m}$$

$$= Tm\frac{\left[V^L - (1 - x_{CO_2})V_u^S\right] - x_{CO_2}V_{CO_2}^V}{(1 - x_{CO_2})\bar{H}_u^L + x_{CO_2}\bar{H}_{CO_2}^L - (1 - x_{CO_2})\bar{H}_u^S - x_{CO_2}\bar{H}_{CO_2}^V} \quad \textbf{(1)}$$

Where V means the molar volume and H molar enthalpy in solid, liquid and vapor phase. A method based on the Clapeyron equation for two components, for predicting the depression of melting temperature for semicrystalline polymer in the presence of CO_2 has been developed for numerous authors in literature[18,21]. Equation (1) could be simplified

152 correctly when the compressed CO_2 and the polymer are immiscible. The simplification of
153 the Clapeyron equation citied by Zhuoyang Lian et al. [18] are shown in Table 1. The value
154 of ΔH_u^{fusion} for the monomeric unit of polyethylene glycol is available in literature, as well
155 as Henry's constant [21].

156 **Table 1.**

<table>
<tr><th colspan="3">**Modification of Clausius Clapeyron Equation (1) to determine T_m at low pressures** [18]</th></tr>
<tr><th colspan="2">**Volume contributions (numerator)**</th><th>**Enthalpy contributions (denominator)**</th></tr>
<tr><td colspan="2">At low pressure the molar volumes of the condensed phases are smaller than the vapor phases.</td><td>Denominator was assumptions the enthalpy, with addition and rest of term; $\left(1-x_{CO_2}\right)\bar{H}_u^*$, where $\bar{H}_u^*$ is the partial molar enthalpy per polymer unit for a pure polymer melt at the same conditions (P,T) as the three-phase equilibrium- Thus, denominator can be expressed in terms of molar heat of fusion per unit of polymer as;</td></tr>
<tr><td colspan="2">$\left[V^L-(1-x_{CO_2})V_u^S\right]\gg 0$</td><td>$\left(1-x_{CO_2}\right)[\bar{H}_u^L-\bar{H}_u^*]+x_{CO_2}\left[\bar{H}_{CO_2}^L-\bar{H}_{CO_2}^V\right]+\left(1-x_{CO_2}\right)\Delta H_u^{fusion}$</td></tr>
<tr><td colspan="2">$x_{CO_2}V_{CO_2}^V\ll 0$</td><td>Commonly, $\Delta H_u^{fusion}\gg\left(1-x_{CO_2}\right)[\bar{H}_u^L-\bar{H}_u^*]+x_{CO_2}\left[\bar{H}_{CO_2}^L-\bar{H}_{CO_2}^V\right]$</td></tr>
<tr><td>x_{CO_2}</td><td>It was determined with the Henry's Equation.; $x_{CO_2}=k_HP$</td><td>$x_{CO_2}\ll 1$</td></tr>
</table>

$V_{CO_2}^V$	It was determined with de compressibility factor, where Z=1; $V_{CO_2}^V = \left({ZRT_m}/{P}\right)$	The denominator can be approximated at low pressure as ΔH_u^{fusion}
$\frac{dT_m}{dP} \approx \frac{-T_m^2 R k_H}{\Delta H_u^{fusion}}$ **(2)**		

157

158 **2.2.2. Sorption of CO_2 in mPEG-alkyne.**

159 For determining the sorption of CO_2 in mPEG-alkyne, high-pressure variable volume cell
160 was used, Figure 2.

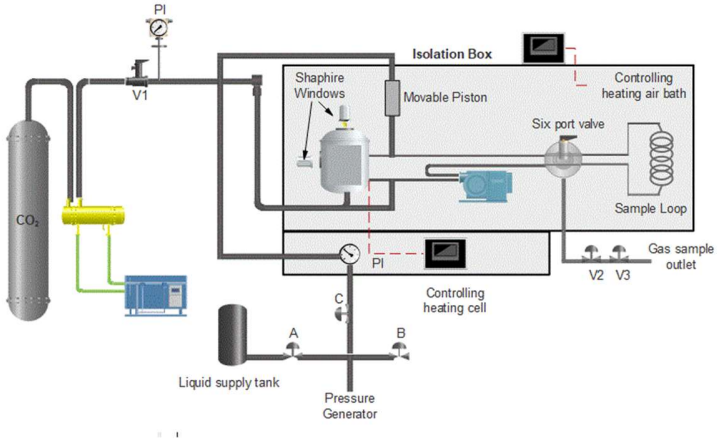

161

162 **Figure 2.**

163 Cell model was ProVis 500 from Eurotechnica, and the equipment consists of a variable-
164 volumen cell, supplied with a front and upper sapphire windows and light for visual
165 observation of phase separation. The cell has a capacity of 50 cm^3 and contains a piston
166 system consisting in a manual pressure generator, a cylinder and a movable piston to avoid
167 pressure drops only when the samples are taken. The cell was filled with 70 mg of mPEG-

168 alkyne and heated to the desired temperature. The volume of cell was determined with the
169 ρ_{CO_2} (CO_2 density) and amount of CO_2 inside of cell. A detail description of the devise can
170 be found in the literature [39].

171 In this study, the sorption measurement was carried out with ex situ gravimetric method, in
172 which the sample is saturated of CO_2 until the equilibrium condition. The time for reaching
173 phase equilibrium was determined by several preliminary experiments, in which samples
174 were taken after 30, 120, 300, 600, 1440 min, as indicated in the supplementary data (Figure
175 S1). After allowing the polymer to saturate with CO_2 the cell was depressurized. The sample
176 was immediately removed from the cell and the weight drop was followed using an analytical
177 balance with accuracy $\pm$0.0001 g.

178 The weight gain of the mPEG-alkyne due to sorption of CO_2, was obtained after 300 minutes
179 and was determined with three mathematical methods of extrapolations: Euler-Romber
180 method, trapezoidal rule and midpoint rule [40]. The equilibrium solubility was calculated
181 as mass of CO_2 absorbed per gram of mPEG-alkyne, as indicated the equation (3).

182 From the equation (4) and knowing w_o, weight of polymer before pressurization process, the
183 weight of mPEG-alkyne was determined. The CO_2 mass fraction was determined with
184 equation (5) and ρ_{CO_2} was determined with the Equation of Bender[41], with SL EOS and
185 with the NIST database (Figure S2). These data are checked by volumetric measurements,
186 which consist on the saturation of polymer in a previously calibrated crucible. When the
187 equilibrium is reached, the crucible is vented, and the volume of CO_2 is measured through a
188 turbine flowmeter.

$$S\ (wt.fraction) = \frac{(wt.of\ CO_2\ inside\ cell)_{P,T}}{(wt.of\ mPEG - alkyne\ )_{P,T;t=0}} \quad \textbf{(3)}$$

$$(wt.of\ mPEG - alkyne\ )_{P,T;t=0} = w_f(T,P) - w_o(T,P) \quad \textbf{(4)}$$

$$(wt.of\ CO_2 inside\ cell)_{P,T} = \rho_{CO_2}(T,P) * Volumen\ of\ the\ cell \quad \textbf{(5)}$$

189

190 ▪ **Henry Law**

191 The polymer/scCO$_2$ mixture undergoes throughout different states, being the first one a liquid
192 or rubbery state, where the absorption of CO$_2$ into the polymer generally follows Henry's law
193 as shown in equation (6). In this law the mass fraction of CO$_2$ absorbed (w_{CO_2}) is proportional
194 to the partial pressure of the scCO$_2$, P_{CO_2}. It is easy to find in literature the Henry's Constant
195 value (k_H) for many polymers, being in this case the k_H value for PEG 0.0198
196 wt.fraction/MPa [21].

$$w_{CO_2} = k_H P_{CO_2} \quad \textbf{(6)}$$

197 ▪ **Dual-Mode Sorption**

198 The dual mode sorption model, equation (7), is a combination of Henry's law in the
199 equilibrium zone and Langmuir type sorption in the non-equilibrium zone. Henry's constant
200 has the same physical meaning for glassy polymers than for rubbery polymers and liquids,
201 whereas the Langmuir-type term account for gas sorption into interstitial spaces and
202 microvoids, which are consequences of local heterogeneities and are intimately related to the
203 slow relaxation processes associated with the glassy state of the polymers.

$$S = k_H P + \frac{c'_H b P}{1 + bP} \quad \textbf{(7)}$$

Where S is the sorption of CO_2 in the polymer, k_H is analogous to Henry's law constant, P is the pressure, c'_H is the saturation of the cavities and b represents the affinity between the solute molecules and the Langmuir sites present in the polymeric matrix. For this work the values of c'_H and b were determined with an Excel spreadsheet tool (Solver system). This system used the nonlinear programming algorithm generalized reduced gradient (GRG).

- **Sanchez-Lacombe equation of state (SL EOS).**

The SL model is based on a lattice theory in which the lattice contains occupied and unoccupied sites, with the sites volume being based on the components [42–45]. A detailed description of the SL EOS can be found in the literature. The equation of state for pure fluids is shown below:

$$\tilde{\rho}^2 + \tilde{P} + \tilde{T}\left[ln(1-\tilde{\rho}) + \left(1 - \frac{1}{r}\right)\tilde{\rho}\right] = 0 \quad \textbf{(8)}$$

$$\tilde{P} = \frac{P}{P^*}, \tilde{T} = \frac{T}{T^*}, \tilde{\rho} = \frac{\rho}{\rho^*}, \rho^* = \frac{\bar{M}}{v^*}, r = \frac{v^* M P^*}{R T^*} \quad \textbf{(9)}$$

where $\tilde{\rho}$, $\tilde{P}$ and $\tilde{T}$ are the reduced density, pressure and temperature, respectively; and ρ^*, P^* and T^* are the characteristic parameters for the pure substance. The size parameter is r, which represent the number of lattice sites occupied by a molecule. R is the gas constant and M is the average molecular weight. For the mixtures, these parameters are determined using a mixing rule:

$$\varphi_1^o = \frac{\varphi_1}{\varphi_1 + \left(v_1^*/v_2^*\right)\varphi_2};\ \varphi_1^o + \varphi_2^o = 1 \quad \textbf{(10)}$$

$$\varphi_1 = \frac{\frac{m_1}{\rho_1^*}}{\frac{m_1}{\rho_1^*} + \frac{m_2}{\rho_2^*}};\ \varphi_1 + \varphi_2 = 1 \quad \textbf{(11)}$$

$$P^* = \varphi_1 P_1^* + \varphi_2 P_2^* - \left(\frac{RT}{v^*}\right)\varphi_1\varphi_2 X_{12} \quad \textbf{(12)}$$

$$P_{12}^* = P_1^* + P_2^* - 2(P_1^* P_2^*)^{\frac{1}{2}}(1 - k_{12})\frac{v^*}{RT} \quad \textbf{(13)}$$

$$T^* = \frac{P^* v^*}{R} \quad \textbf{(14)}$$

$$r = x_1 r_1 + x_2 r_2;\ x_1 + x_2 = 1 \quad \textbf{(15)}$$

$$\frac{1}{\rho^*} = \frac{m_1}{\rho_1^*} + \frac{m_2}{\rho_2^*} \quad \textbf{(16)}$$

where m_1 is the mass fraction of the component CO_2 in the mixtures, k_{12} is a binary interaction parameter and x_1 and x_2 are the mole fractions of the mixture. The superscript * indicates that the parameter corresponds to the binary mixture, the subscript 1 stands for CO_2 and 2 for polymer. The binary interaction parameter, k_{12}, between the polymer and CO_2 is needed to calculate the characteristic parameters of mixture.

When the polymer/gas mixture reaches a state of equilibrium at operating temperature and pressure, the chemical potentials of the CO_2 should be the same at the interface between the gas phase and polymer/gas mixture. That means, the last equation required for solubility calculations is the phase balance equation, which equals the chemical potentials of the gas in two phases.

$$\mu_1^G(T,P) = \mu_1^P(T,P,m_1) \tag{17}$$

$$\frac{\mu_1^P}{RT} = ln\varphi_1 + \left(1 - \frac{r_1}{r_2}\right)\varphi_2 + r_1\tilde{\rho}X_{12}\varphi_2^2\frac{v_1^*}{v^*} + r_1\left[\frac{-\tilde{\rho} + \tilde{P}_1\tilde{v}}{\tilde{T}_1} + \tilde{v}\left((1-\tilde{\rho})\ln(1-\tilde{\rho}) + \frac{\tilde{\rho}ln\tilde{\rho}}{r_1}\right)\right] \tag{18}$$

$$\frac{\mu_1^G}{RT} = r_1\left[\frac{-\tilde{\rho}_1 + \tilde{P}_1\tilde{v}_1}{\tilde{T}_1} + \tilde{v}_1\left((1-\tilde{\rho}_1)\ln(1-\tilde{\rho}_1) + \frac{\tilde{\rho}_1 ln\tilde{\rho}_1}{r_1}\right)\right] \tag{19}$$

Where the superscripts G and P represent the gas and the polymer/CO_2 mixture, respectively. The gas phase is assumed to be a pure gas, because of the low volatility of high molecular weight of polymer. There are numerous sources of characteristic parameters available in the literature, in this work the characteristic parameters that offer the best correlation for sorption data are shown in Table 2. In the supporting material, the characteristic parameters for CO_2 with SL EOS were estimated (Table S1 and Figure S2)[46].

Table 2.

	P* MPa	ρ* g/cm3	T* Kelvin	Ref.
CO_2	338.7	1.4055	338.7	[47]
PEG	635.7	1.11832	635.5	[48],[49]

- **Heuristic Model**

A heuristic model with experimental data has been correlated by Pasquali et al.[27] following the models proposed by Giddings et al. [50,51], where the solubility parameter can be

240 expressed as a function of the CO_2 solubility parameter and fitted by a second-degree
241 equation:

$$\log X = a\delta^2 + b\delta + C \quad \textbf{(20)}$$

242 where X is the solute mole fraction, a and b are coefficients, C is a constant and δ is the
243 solubility parameter of the CO_2 at a given conditions. The solubility parameter of CO_2 can
244 be calculated by the equation:

$$\delta = 1.25 Pc^{1/2} \frac{\rho r}{\rho r(liq)} \quad \textbf{(21)}$$

245 where P_c, is the critical pressure and ρr, is the reduced density, which is the ratio of the
246 apparent density of CO_2 at given pressure and temperature to the critical density of CO_2. The
247 apparent density of CO_2 has been calculated through the Bender equation and NIST (Figure
248 S2). The solubility parameter of mPEG-alkyne was calculated with the Small method of
249 group contributions. These parameters appear in the supporting material in the Table S3.

250 3. Results and Discussion

251 The results have been divided in two sections. In the first place, we report the obtained values
252 for the melting points of mPEG-alkyne under different pressures with the help of HP DSC;
253 and the experimental values were correlated using a Clausius Clapeyron equation. In the
254 second section, the sorption of mPEG-alkyne into $scCO_2$ was determined experimentally at
255 different pressures and at two different temperatures. These measurements were correlated
256 using Henry, Dual model, SL EOS and Heuristic Model and experimental and theoretical
257 data were compared with the results from literature.

3.1. Melting point temperatures of mPEG-alkyne

The influence of CO_2 in the melting temperature of mPEG-alkyne was determined by HP DSC as a function of temperature and/or pressure. The influence of pressure on the melting point temperature is shown in Figure 3, where three different regions can be observed.

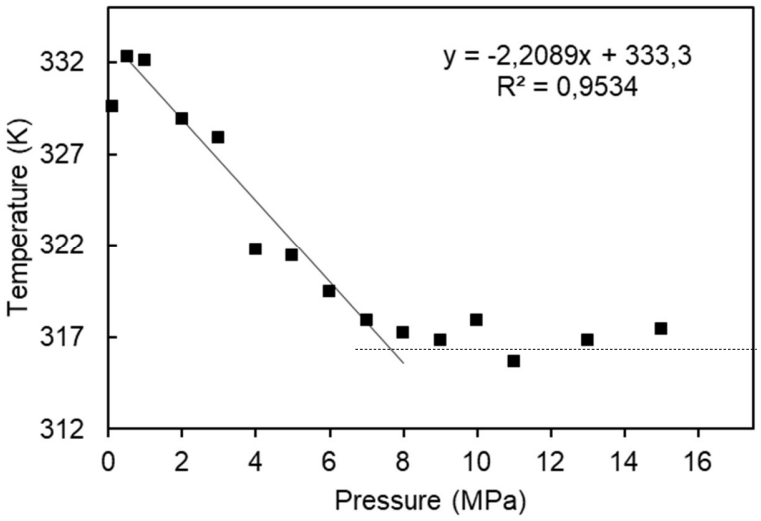

Figure 3.

The first one in the 0.1-0.5 MPa pressure range, where the melting point temperature of mPEG-alkyne started with a value around 329.58 K and then increased very lightly (2.72 K) with higher pressures. The second region shows a linear decrease of the melting point temperature between 1 and 8 MPa, when the critical pressure of CO_2 is reached and the melting point takes a value around 317 K. In the third region, at pressures higher than 8 MPa, an almost constant value of the melting point temperature was observed, with no more influence of the pressure increase in this parameter. The effect observed in the first region could be attributed to the increase of the crystal thickness during the exposure to CO_2. In the second region, a linear decrease of the melting temperature is observed in the range 0.5-8

MPa, (near of critical pressure of CO_2) that can be attributed of the effects of the dissolution of CO_2 into the polymer, which tends to reduce the melting temperature [18].

Linear regression was applied to the experimental data of this region in order to determine, dT_m/dP. The cut-off point was determined by fitting the high pressure data to a straight line with a zero slope. The slope value for the mPEG-alkyne/CO_2 systems was 2.2089 K/MPa. The relationship between the melting point temperature and pressure can be properly described by the Clapeyron equation. Therefore, the experimental slope value was compared to the value predicted by Clausius Clapeyron's equation which was 2.101 K/MPa with a SSE of 0.13%, thus the modification of Clausius Clapeyron describes with accuracy the slope -dT_m/dP for this system.

In addition, it was compared the experimental data of -dT_m/dP reported in literature with the calculated -dT_m/dP, the variation of melting temperature and pressure (Table 3), where a high level of precision of the modified Clausius Clapeyron equation was achieved.

Table 3.

Polymer	**ΔH_f [a] (J/mol)**	**k_H [a] (MPa)**	**$-dT_m/dP_{calc}$ (K/MPa)**	**$-dT_m/dP_{exp}$ (K/MPa)**	**Analytical Method**	**SSE (%)**	**Ref.**
mPEG-alkyne,2 kDa	8.29	0.0198	2.10	2.21	HP DSC	0.13	This work
PEG,4 kDa	8.29	0.0198	2.22	2.22	HP View cell	3.9E-6	[27]
PEG, 35 kDa	8.29	0.0198	1.93	1.57	HP View cell	10.89	[20]
PEG, 35 kDa	8.29	0.0198	1.90	1.3	HP DSC	39.69	[20]

[a]Data found in literature [21,52].

A comparison between experimental data and those reported in the literature are shown in Figure 4.

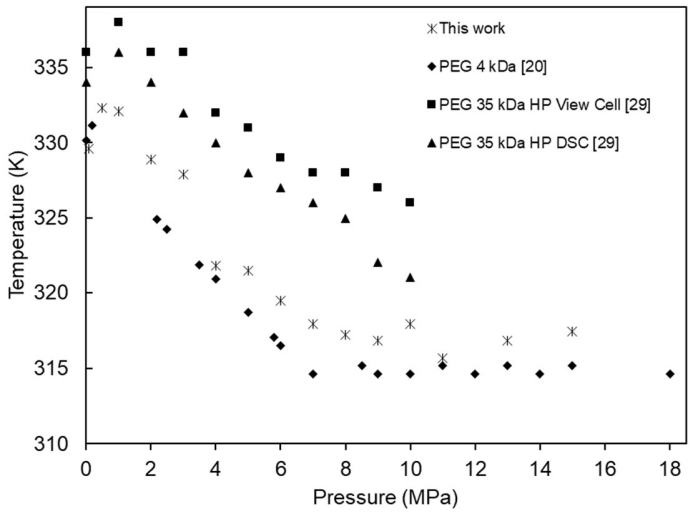

Figure 4.

The results of Pasquali et al. [27] and results of Knez [20] present the same shape of data obtained in this work. Results for a PEG with a molecular weight of 4000 $g \cdot mol^{-1}$ showed similar initial melting temperature value (330 K) and a similar slope of the curve in the region of moderate pressure (1 MPa to 8 MPa) than the ones reported in our work. Surprisingly, the values obtained in our measurements for the mPEG-alkyne are over the results reported by Pasquali et al [27]. However, big differences between the PEG 35000 $g \cdot mol^{-1}$ data of Knez et al. [20] and the data of this work has been observed. This shift is due to the melting point strongly depends on the molecular weight of the PEG considered, showing higher values with increasing molecular weight [53–55]. Moreover, the shift can be assigned to a different initial T_m value at ambient pressure.

The melting temperature of mPEG 2000 g·mol^{-1} is K and 329.58 K of mPEG-alkyne at 80 MPa. This finding showed that the presence of a single alkyne group did not have a strong influence on the crystallization ability of the PEG, but the presence of the alkyne group make the polymer less compatible with the CO_2 [56].

In addition, it is worth mentioning that the differences of the reported data might be explained considering the different analytical methods. A review of the different measurement methods and the experimental results on melting temperature depression of PEG 35000 in CO_2 atmosphere has been published by Knez et al. [20] and Pasquali et al. [28], who studied the depression of melting point for PEG 1500 and 4000 g·mol^{-1} using a capillary method in a high pressure optical cell. Extensive research has been done on the experimental determination of the melting point for the PEG/CO_2 mixture, showing the capillary method in a high pressure optical cell some advantages as it is an inexpensive technique for determining basic design data. However, HP DSC is a faster method for determining this parameter and the systematic error done by the researcher could be diminished.

3.2. Sorption of CO_2 into mPEG-alkyne

According to literature, polymers with high molecular weight are generally insoluble in CO_2. On the other hand, the solubility of high pressure CO_2 into the polymer matrix use to be high for most of the polymers and is one the most important properties of the scCO2-assited polymer processing, especially for making foams, micro-nanoparticles or microcapsules into $scCO_2$. The plasticisation of polymer results from sorption of CO_2 into polymer matrix under pressure. But plasticisation affects not only to the melting point as has been pointed out in the previous section, affect the Tg of the polymer as well, lowering this value and getting the

swelling polymer less viscous thanks to the CO_2 embedded in the range of pressure and temperature between Tg and melting point. According to the previous section, the melting point of mPEG-alkyne with 2000 $g \cdot mol^{-1}$ is between 317 and 336 K, so it is quite unfavourable to measure the solubility below this temperature range because the polymer is not in liquid state [53]. Hence, sorption of supercritical carbon dioxide in mPEG-alkyne was measured at pressures up to 17 MPa and at 308 and 318 K, as shown in Figure 5.

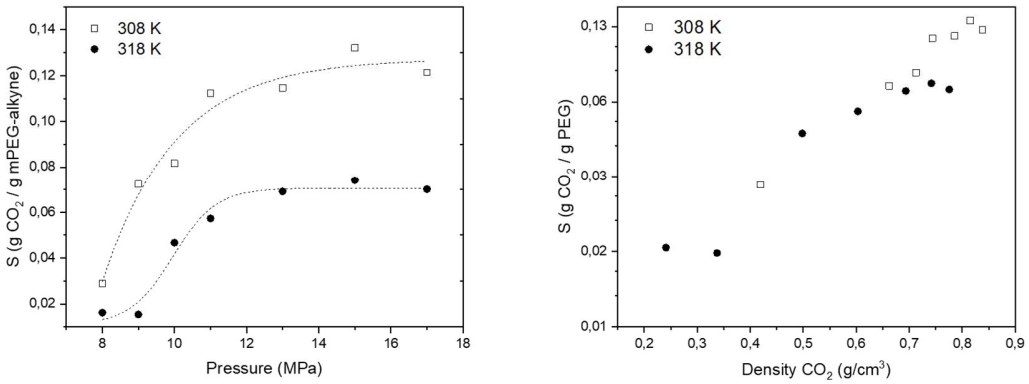

Figure 5.

The solubility values observed at low pressure are related with the presence of the crystallin phase. In this region, the penetration of the CO_2 into the packed chains of polymer could be close to zero. The Figure 3 (left) shows that the sorption increases linearly up to 11 MPa for both temperatures. From there, the sorption of CO_2 reaches a constant value which is different for each temperature. This effect has been previously discussed in literature [17,24,31,57]. As shown in Figure 5 (right), where the solubility data are plot against the density of CO_2, the data follow a single curve with no observable temperature effect, because the diffusion power of CO_2 increases with higher densities [58]. This trend has been generally observed in many gas/ polymer systems, when density increases the gas molecules are forced between

polymer chains, expanding the space between molecules and thus increasing their mobility. In addition, increased mobility of the chains allows a higher amount of CO_2 to be absorbed into the polymer phase. One can notice that, the pressure increase or a temperature decrease favour the sorption upgrade and therefore for the possibility of using supercritical fluids for processing polymers.

The behaviour of supercritical CO_2 mPEG-alkyne system was also predicted by using a Henry model, a Dual Mode, a Sanchez Lacombe EOS (Figure 6) and Heuristic model (Figure 7).

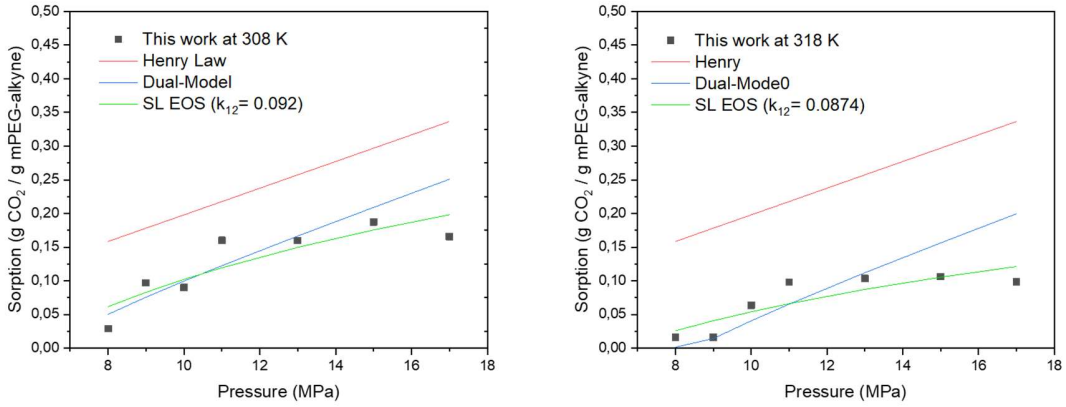

Figure 6.

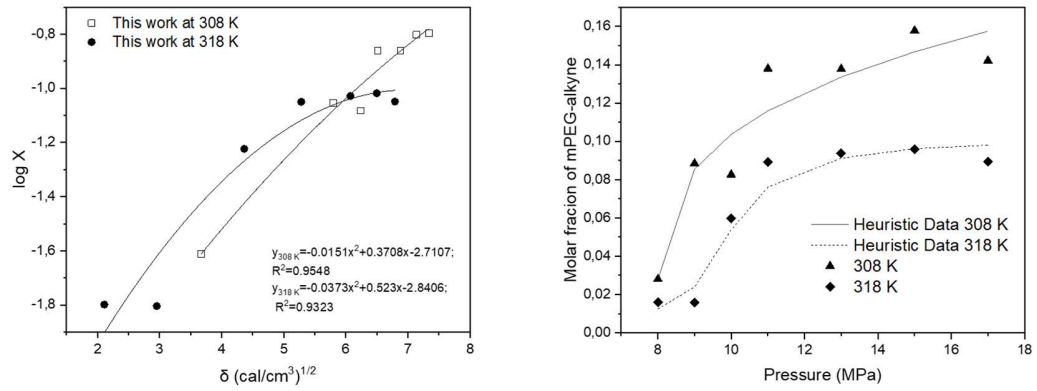

353 **Figure 7.**

354 At low pressures, Henry's model can be used to accurately describe the pressure dependence
355 of the sorption through the dissolution process. However, this model is only reliable at low
356 pressure so in this study this model does not offer a good fit since the pressure range studied
357 is higher than 7 MPa. Dual Mode, which is a combination of Henry's Law and Langmuir
358 type sorption, shown a better fit at high pressure as it takes into account gas sorption into
359 interstitial spaces and microvoids, which are consequences of local heterogeneities and are
360 intimately related to the slow relaxation processes associated with the glassy state of the
361 polymers [59]. It is observed that SL EOS predicts the experimental data with reasonable
362 accuracy and improves the results shown by the Dual-Mode model. The modelling results of
363 Sanchez Lacombe and Dual Mode shown the reliability for predicting the phase behaviour
364 of the system at high pressures.

365 According to the heuristic model, when the solubility parameter calculated with the group
366 contributions method [21,60] of two substances is similar, the solubilization is promoted. In
367 this case, the difference between the parameters of $scCO_2$ and m-PEG-alkyne warrants low
368 solubilization. In the supporting material the density values, solubility parameters of mPEG-
369 alkyne at 308 K at 318 K are shown in Table S2. The solubility parameter of mPEG-alkyne
370 was calculated with the Small method of group contribution as 17.6082 $MPa^{1/2}$ or 8.8041
371 $cal^{1/2}cm^{-3/2}$. The Figure 7 (left) depicts the logarithm of mPEG-alkyne molar fraction versus
372 the CO_2 solubility parameter (δ). The data obtained was adjusted to a second degree
373 polynomial equation according to equation (20). The maximum value of the two curves at
374 308 K has a value of 8.649 and 7.011 at 318 K, values close to the solubility parameter of
375 mPEG-alkyne calculated by the method of group contributions.

376 Knowing the coefficient, a and b and the constant C, the solubility of mPEG-alkyne in CO_2
377 was calculated with the equation (21), all values are shown in Figure 7 (right). Figure 7 (right)
378 compares the heuristic model and experimental data and it is observed that this model
379 correlates the experimental data with reasonable accuracy.

380 Finally, the sorption data collected were compared with those reported in works published
381 recently using operations conditions close to those selected in this work. Elena Aionicesei et
382 al. [48] and Pasquali et al. [28] studied the solubility of system CO_2/PEG 1500 $g \cdot mol^{-1}$ at 323
383 K and 308-328 K, respectively, and in a range up to 17 MPa. The differences in solubility
384 measurement results found between this work and literature are acceptable, especially when
385 we know that there is an appreciable difference between the two literature results themselves
386 as shown in Figure 8.

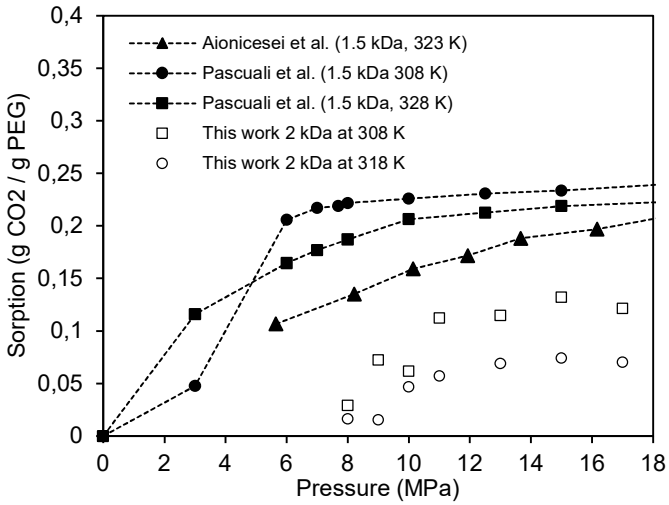

387

388 **Figure 8.**

389 Note, the variation between Pascuali et al. [28] data at temperature of 308 K and data
390 reported in this study at the same temperature is 0.1 g CO_2/ g PEG at high pressure. The
391 differences observed for the sorption capacity of supercritical CO_2 can be mainly attributed

to molecular weight of PEG, as the experiments compared employed a PEG of 1500 g·mol^{-1}. Solubility of PEG 1500 and PEG 2000 are close to each other in values and both data from Aionicesei and Pascuali, as reported in this paper, follow almost the same trend. In addition, the effects of the molecular weight of PEGs on carbon dioxide was determined by Gregor Kravanja et al. [25], and the difference between a PEG of 1500 g·mol^{-1} and 3000 g·mol^{-1} at 15 MPa was 0.1 g CO_2 absorbance in PEG and 0.19 g CO_2 in PEG at 20 MPa. The differences can also be associated with the use of different analytical methods. According to Maša Knez Hrnčič et al. [26], the solubility values obtained by external balance method and Magnetic Suspense Balance (MSB) showed an absolute average relative deviation (AARD) of up to 54% in a range of 15 MPa, which explains the solubility values obtained are much lower than the data compared.

4. Conclusions

The study of melting point provides information on the pressure required to melt the polymer and to produce a saturated liquid solution, which is a parameter of major importance, especially for the preparation of a conjugated drug-polymer in scCO_2. The sorption of CO_2 into the polymer leads to a reduction of the melting point and it was determined by HP DSC. The melting temperature curve of mPEG has a maximum at 0.5 MPa and a minimum at 8 MPa, keeping this value also at higher pressures. A difference of about 16.6 K was observed between the maximum and minimum of the melting temperature curve, with a slope $-dT_m/dP$ of 2.2089 K/MPa in the linear region, value similar to that obtained with the Clausius Clapeyron modified equation.

Sorption of CO_2 in mPEG-alkyne increases with pressure and decreases with increasing temperature. The experimental data obtained for CO_2 and mPEG-alkyne is in good agreement

415 with other experimental results observed in literature for the system CO_2 - PEG, thus the
416 terminal alkyne groups have not a significant effect in the phase behaviour of the system.
417 The experimental data were correlated using the Henry Law, Dual-Mode, Sanchez Lacombe
418 equation of state and the heuristic model. Henry Law model is reliable at low pressure so in
419 this study this model does not offer a good fit since the pressure range studied is higher than
420 7 MPa. The modelling results of Sanchez Lacombe and Dual Mode shown the reliability for
421 predicting the phase behaviour of the system at high pressures and finally, heuristic model is
422 an affordable and easy to apply model, with a great fit.

423

424 5. Acknowledgments

425 We gratefully acknowledge funding from the Ministry of economy and competitiveness
426 through funding the projects Ref. CTQ2016-79811-P. The authors also acknowledge the
427 support of the Ministry of economy and competitiveness for the fellowship of Ms. López
428 Quijorna Ref. BES-2017-079770. The authors state that they have not conflict of interest
429 with any public or private body.

430

431 6. Supporting Information Available

432 In the supporting material the experimental results for evaluating the saturation time of
433 mPEG-alkyne in $scCO_2$, the algorithm for solving SL EOS, the choice of characteristic
434 parameters used to carry out the SL EOS calculations and the determination of the solubility
435 parameter of mPEG-alkyne with the group's contribution method.

436

437 **Figure captions**

438 **Figure 1.** Schematic diagram of high-pressure differential scanning calorimetry for the
439 measurement of the melting point.

440 **Figure 2**. Schematic diagram of the variable high-pressure view cell for sorption
441 measurements.

442 **Figure 3.** Variation of the melting temperature of mPEG-alkyne as a function of CO_2
443 pressure.

444 **Figure 4.** Melting temperature of PEG as a function of CO_2 pressure. Lines are added as a
445 guide to the eye.

446 **Figure 5.** (Left) CO_2 sorption in mPEG-alkyne as a function of pressure at different
447 temperatures (Right) CO_2 sorption in mPEG-alkyne as a function of density of CO_2
448 determined with the equation of Bender.

449 **Figure 6.** Sorption experimental data of CO_2 in mPEG-alkyne at (left) 308 K and at (right)
450 318 K. Correlation of experimental data using Henry's Law (--), Dual-Model (--) and SL
451 EOS (--).

452 **Figure 7.** Heuristic Model: (left figure) logarithm of mPEG-alkyne mole fraction vs. the CO_2
453 solubility parameter, (right figure) correlation of data calculated with Heuristic Model and
454 experimental data.

455 **Figure 8.** Comparison between the experimental data obtained in this work and those from
456 the literature as it is indicated by the markers.

457

458 **Table Captions**

459 **Table 1.** Summary of the modifications made to the Clausius Clapeyron equation to
460 determine $-dT_m/dP$ at low pressure.

461 **Table 2.** SL EOS characteristic parameters for CO_2 and PEG.

462 **Table 3.** Summary of the modifications made to the Clausius Clapeyron equation to
463 determine $-dT_m/dP$ at low pressure.

References.

[1] J. Harris, R. Chess, Effect of PEGylation on pharmaceuticals, Nat. Rev. Drug Discov. 2 (2003) 214–221. https://doi.org/10.1038/nrd1033.

[2] A. Bunker, Poly(Ethylene Glycol) in Drug Delivery, Why Does it Work, and Can We do Better? All Atom Molecular Dynamics Simulation Provides Some Answers, Phys. Procedia. 34 (2012) 24–33. https://doi.org/https://doi.org/10.1016/j.phpro.2012.05.004.

[3] A.A. D'souza, R. Shegokar, Polyethylene glycol (PEG): a versatile polymer for pharmaceutical applications, Expert Opin. Drug Deliv. 13 (2016) 1257–1275. https://doi.org/10.1080/17425247.2016.1182485.

[4] A. Thomas, S.S. Müller, H. Frey, Beyond Poly(ethylene glycol): Linear Polyglycerol as a Multifunctional Polyether for Biomedical and Pharmaceutical Applications, Biomacromolecules. 15 (2014) 1935–1954. https://doi.org/10.1021/bm5002608.

[5] M. Zacchigna, F. Cateni, S. Drioli, G.M. Bonora, Multimeric, Multifunctional Derivatives of Poly(ethylene glycol), Polymers (Basel). 3 (2011) 1076–1090. https://doi.org/10.3390/polym3031076.

[6] M.R. Sherman, L.D. Williams, M.A. Sobczyk, S.J. Michaels, M.G.P. Saifer, Role of the Methoxy Group in Immune Responses to mPEG-Protein Conjugates, Bioconjug. Chem. 23 (2012) 485–499. https://doi.org/10.1021/bc200551b.

[7] M.M. Velencoso, A.S.B. Gonzalez, J.C. García-Martínez, M.J. Ramos, A. De Lucas, J.F. Rodriguez, Click-ligation of coumarin to polyether polyols for polyurethane foams, Polym. Int. 62 (2013) 783–790. https://doi.org/10.1002/pi.4363.

[8] H.C. Kolb, K.B. Sharpless, The growing impact of click chemistry on drug discovery, Drug Discov. Today. 8 (2003) 1128–1137. https://doi.org/https://doi.org/10.1016/S1359-6446(03)02933-7.

[9] Y. Shi, X. Cao, H. Gao, The use of azide–alkyne click chemistry in recent syntheses and applications of polytriazole-based nanostructured polymers, Nanoscale. 8 (2016) 4864–4881. https://doi.org/10.1039/C5NR09122E.

[10] M.J. Arévalo, Ó. López, M.V. Gil, Green Chemical Synthesis and Click Reactions, in: Click React. Org. Synth., John Wiley & Sons, Ltd, 2016: pp. 77–97. https://doi.org/10.1002/9783527694174.ch3.

[11] M. van Dijk, D.T.S. Rijkers, R.M.J. Liskamp, C.F. van Nostrum, W.E. Hennink, Synthesis and Applications of Biomedical and Pharmaceutical Polymers via Click Chemistry Methodologies, Bioconjug. Chem. 20 (2009) 2001–2016. https://doi.org/10.1021/bc900087a.

[12] V. Crescenzi, L. Cornelio, C. Di Meo, S. Nardecchia, R. Lamanna, Novel Hydrogels via Click Chemistry: Synthesis and Potential Biomedical Applications, Biomacromolecules. 8 (2007) 1844–1850. https://doi.org/10.1021/bm0700800.

[13] K. Nwe, M. Brechbiel, Growing Applications of "Click Chemistry" for Bioconjugation in Contemporary Biomedical Research, Cancer Biother. Radiopharm. 24 (2009) 289–302. https://doi.org/10.1089/cbr.2008.0626.

[14] T. Kegl, G. Kravanja, Ž. Knez, M.K. Hrnčič, Effect of addition of supercritical CO2 on transfer and thermodynamic properties of biodegradable polymers PEG 600 and Brij52, J. Supercrit. Fluids. 122 (2017) 10–17.

https://doi.org/https://doi.org/10.1016/j.supflu.2016.11.011.

[15] C.F. Kirby, M.A. McHugh, Phase Behavior of Polymers in Supercritical Fluid Solvents, Chem. Rev. 99 (1999) 565–602. https://doi.org/10.1021/cr970046j.

[16] P.J. Ginty, M.J. Whitaker, K.M. Shakesheff, S.M. Howdle, Drug delivery goes supercritical, Mater. Today. 8 (2005) 42–48. https://doi.org/https://doi.org/10.1016/S1369-7021(05)71036-1.

[17] E. Weidner, V. Wiesmet, Ž. Knez, M. Škerget, Phase equilibrium (solid-liquid-gas) in polyethyleneglycol-carbon dioxide systems, J. Supercrit. Fluids. 10 (1997) 139–147. https://doi.org/https://doi.org/10.1016/S0896-8446(97)00016-8.

[18] Z. Lian, S.A. Epstein, C.W. Blenk, A.D. Shine, Carbon dioxide-induced melting point depression of biodegradable semicrystalline polymers, J. Supercrit. Fluids. 39 (2006) 107–117. https://doi.org/https://doi.org/10.1016/j.supflu.2006.02.001.

[19] S. Takahashi, J.C. Hassler, E. Kiran, Melting behavior of biodegradable polyesters in carbon dioxide at high pressures, J. Supercrit. Fluids. 72 (2012) 278–287. https://doi.org/https://doi.org/10.1016/j.supflu.2012.09.009.

[20] Ž. Knez, M. Škerget, Z. Mandžuka, Determination of S–L phase transitions under gas pressure, J. Supercrit. Fluids. 55 (2010) 648–652. https://doi.org/https://doi.org/10.1016/j.supflu.2010.09.016.

[21] G.C. Martin, Physical Properties of Polymers Handbook, 2nd ed Edited by James E. Mark (University of Cincinnati, OH). Springer Science + Business Media, LLC: New York. 2007. xx + 1076 pp. $349.00. ISBN 978-0-387-31235-4., J. Am. Chem. Soc. 130 (2008) 1111. https://doi.org/10.1021/ja0769503.

530 [22] E. de Paz, Á. Martín, S. Rodríguez-Rojo, J. Herreras, M.J. Cocero, Determination of
531 Phase Equilibrium (Solid−Liquid−Gas) in Poly-(ε-caprolactone)−Carbon Dioxide
532 Systems, J. Chem. Eng. Data. 55 (2010) 2781–2785.
533 https://doi.org/10.1021/je900997t.

534 [23] Z. Zhang, Y.P. Handa, CO2-Assisted Melting of Semicrystalline Polymers,
535 Macromolecules. 30 (1997) 8505–8507. https://doi.org/10.1021/ma9712211.

536 [24] V. Wiesmet, E. Weidner, S. Behme, G. Sadowski, W. Arlt, Measurement and
537 modelling of high-pressure phase equilibria in the systems polyethyleneglycol (PEG)–
538 propane, PEG–nitrogen and PEG–carbon dioxide, J. Supercrit. Fluids. 17 (2000) 1–
539 12. https://doi.org/https://doi.org/10.1016/S0896-8446(99)00043-1.

540 [25] G. Kravanja, M.K. Hrnčič, M. Škerget, Ž. Knez, Interfacial tension and gas solubility
541 of molten polymer polyethylene glycol in contact with supercritical carbon dioxide
542 and argon, J. Supercrit. Fluids. 108 (2016) 45–55.
543 https://doi.org/https://doi.org/10.1016/j.supflu.2015.10.013.

544 [26] M.K. Hrnčič, E. Markočič, N. Trupej, M. Škerget, Ž. Knez, Investigation of
545 thermodynamic properties of the binary system polyethylene glycol/CO2 using new
546 methods, J. Supercrit. Fluids. 87 (2014) 50–58.
547 https://doi.org/https://doi.org/10.1016/j.supflu.2013.12.021.

548 [27] I. Pasquali, L. Comi, F. Pucciarelli, R. Bettini, Swelling, melting point reduction and
549 solubility of PEG 1500 in supercritical CO2, Int. J. Pharm. 356 (2008) 76–81.
550 https://doi.org/https://doi.org/10.1016/j.ijpharm.2007.12.048.

551 [28] I. Pasquali, J.-M. Andanson, S.G. Kazarian, R. Bettini, Measurement of CO2 sorption

552 and PEG 1500 swelling by ATR-IR spectroscopy, J. Supercrit. Fluids. 45 (2008) 384–
553 390. https://doi.org/https://doi.org/10.1016/j.supflu.2008.01.015.

554 [29] M. Daneshvar, S. Kim, E. Gulari, High-pressure phase equilibria of polyethylene
555 glycol-carbon dioxide systems, J. Phys. Chem. 94 (1990) 2124–2128.
556 https://doi.org/10.1021/j100368a071.

557 [30] D. Gourgouillon, M. da Ponte, High pressure phase equilibria for poly(ethylene
558 glycol)s + CO2: experimental results and modelling, Phys. Chem. Chem. Phys. 1
559 (1999) 5369–5375. https://doi.org/10.1039/A906927E.

560 [31] I. Álvarez, C. Gutiérrez, A. [de Lucas], J.F. Rodríguez, M.T. García, Measurement,
561 correlation and modelling of high-pressure phase equilibrium of PLGA solutions in
562 CO2, J. Supercrit. Fluids. 155 (2020) 104637.
563 https://doi.org/https://doi.org/10.1016/j.supflu.2019.104637.

564 [32] C. Gutiérrez, J.F. Rodríguez, I. Gracia, A. de Lucas, M.T. García, Foaming Process
565 from Polystyrene/p-Cymene Solutions Using CO2, Chem. Eng. Technol. 37 (2014)
566 1845–1853. https://doi.org/10.1002/ceat.201300780.

567 [33] A. Kolate, D. Baradia, S. Patil, I. Vhora, G. Kore, A. Misra, PEG — A versatile
568 conjugating ligand for drugs and drug delivery systems, J. Control. Release. 192
569 (2014) 67–81. https://doi.org/https://doi.org/10.1016/j.jconrel.2014.06.046.

570 [34] Y.K. Chong, I. Zainol, C.H. Ng, I.H. Ooi, Miktoarm star polymers nanocarrier:
571 synthesis, characterisation, and in-vitro drug release study, J. Polym. Res. 26 (2019)
572 79. https://doi.org/10.1007/s10965-019-1726-4.

573 [35] E. Marin, M.I. Briceño, C. Caballero-George, Critical evaluation of biodegradable

574 polymers used in nanodrugs, Int. J. Nanomedicine. 8 (2013) 3071–3090.
575 https://doi.org/10.2147/IJN.S47186.

576 [36] R.G. Wissinger, M.E. Paulaitis, Swelling and sorption in polymer–CO2 mixtures at
577 elevated pressures, J. Polym. Sci. Part B Polym. Phys. 25 (1987) 2497–2510.
578 https://doi.org/10.1002/polb.1987.090251206.

579 [37] Y. Zhang, K.K. Gangwani, R.M. Lemert, Sorption and swelling of block copolymers
580 in the presence of supercritical fluid carbon dioxide, J. Supercrit. Fluids. 11 (1997)
581 115–134. https://doi.org/https://doi.org/10.1016/S0896-8446(97)00031-4.

582 [38] Y. Sato, K. Fujiwara, T. Takikawa, Sumarno, S. Takishima, H. Masuoka, Solubilities
583 and diffusion coefficients of carbon dioxide and nitrogen in polypropylene, high-
584 density polyethylene, and polystyrene under high pressures and temperatures, Fluid
585 Phase Equilib. 162 (1999) 261–276. https://doi.org/https://doi.org/10.1016/S0378-
586 3812(99)00217-4.

587 [39] C. Gutiérrez, J.F. Rodríguez, I. Gracia, A. de Lucas, M.T. García, Modification of
588 polystyrene properties by CO2: Experimental study and correlation, J. Appl. Polym.
589 Sci. 132 (2015). https://doi.org/10.1002/app.41696.

590 [40] L. Lapidus, J.H. Seinfeld, eds., 5 Extrapolation Methods, in: Numer. Solut. Ordinary
591 Differ. Equations, Elsevier, 1971: pp. 242–266.
592 https://doi.org/https://doi.org/10.1016/S0076-5392(08)63012-X.

593 [41] E. Bender, Equations of state for ethylene and propylene, Cryogenics (Guildf). 15
594 (1975) 667–673. https://doi.org/https://doi.org/10.1016/0011-2275(75)90100-9.

595 [42] I.C. Sanchez, R.H. Lacombe, An elementary molecular theory of classical fluids. Pure

596 fluids, J. Phys. Chem. 80 (1976) 2352–2362. https://doi.org/10.1021/j100562a008.

597 [43] I.C. Sanchez, R.H. Lacombe, Statistical Thermodynamics of Polymer Solutions,
598 Macromolecules. 11 (1978) 1145–1156. https://doi.org/10.1021/ma60066a017.

599 [44] C. Panayiotou, I.C. Sanchez, Swelling of network structures, Polymer (Guildf). 33
600 (1992) 5090–5093. https://doi.org/https://doi.org/10.1016/0032-3861(92)90064-4.

601 [45] J. De Pablo, J.D. Schieber, Molecular Engineering Thermodynamics, Cambridge,
602 Cambridge, 2014.

603 [46] C. Wang, On the information and methods for calculation of Sanchez-Lacombe and
604 group-contribution lattice-fluid equations of state, Korean J. Chem. Eng. 23 (2006)
605 102–107. https://doi.org/10.1007/BF02705699.

606 [47] I. Gil'mutdinov, I. Gil'mutdinov, I. Kuznetsova, A. Sabirzyanov, Solubility of
607 supercritical carbon dioxide in polyethylene glycol 4000, High Temp. 54 (2016) 78–
608 81. https://doi.org/10.1134/S0018151X16010028.

609 [48] E. Aionicesei, M. Škerget, Ž. Knez, Measurement and Modeling of the CO2 Solubility
610 in Poly(ethylene glycol) of Different Molecular Weights, J. Chem. Eng. Data. 53
611 (2008) 185–188. https://doi.org/10.1021/je700467p.

612 [49] E. Markočič, M. Škerget, Ž. Knez, Measurement and Modeling of the CO2 Solubility
613 in Poly(ethylene glycol) of Different Molecular Weights, J. Chem. Eng. Data - J
614 CHEM ENG DATA. 53 (2007). https://doi.org/10.1021/je700467p.

615 [50] J.C. Giddings, J.J. Czubryt, M.N. Myers, Solubility phenomena in dense carbon
616 dioxide gas in the range 270-1900 atmospheres, J. Phys. Chem. 74 (1970) 4260–4266.
617 https://doi.org/10.1021/j100718a014.

618 [51] T. Guadagno, S.G. Kazarian, High-Pressure CO2-Expanded Solvents: Simultaneous
619 Measurement of CO2 Sorption and Swelling of Liquid Polymers with in-Situ Near-IR
620 Spectroscopy, J. Phys. Chem. B. 108 (2004) 13995–13999.
621 https://doi.org/10.1021/jp0481097.

622 [52] L. Mandelkern, The Crystallization Of Flexible Polymer Molecules, Chem. Rev. 56
623 (1956) 903–958. https://doi.org/10.1021/cr50011a001.

624 [53] K. Pielichowski, K. Flejtuch, Differential scanning calorimetry studies on
625 poly(ethylene glycol) with different molecular weights for thermal energy storage
626 materials, Polym. Adv. Technol. 13 (2002) 690–696. https://doi.org/10.1002/pat.276.

627 [54] D.O. Corrigan, A.M. Healy, O.I. Corrigan, The effect of spray drying solutions of
628 polyethylene glycol (PEG) and lactose/PEG on their physicochemical properties, Int.
629 J. Pharm. 235 (2002) 193–205. https://doi.org/https://doi.org/10.1016/S0378-
630 5173(01)00990-5.

631 [55] S.P. Nalawade, F. Picchioni, L.P.B.M. Janssen, Supercritical carbon dioxide as a green
632 solvent for processing polymer melts: Processing aspects and applications, Prog.
633 Polym. Sci. 31 (2006) 19–43.
634 https://doi.org/https://doi.org/10.1016/j.progpolymsci.2005.08.002.

635 [56] J. Gregorowicz, Z. Fraś, P. Parzuchowski, G. Rokicki, M. Kusznerczuk, S.
636 Dziewulski, Phase behaviour of hyperbranched polyesters and polyethers with
637 modified terminal OH groups in supercritical solvents, J. Supercrit. Fluids. 55 (2010)
638 786–796. https://doi.org/https://doi.org/10.1016/j.supflu.2010.09.005.

639 [57] G.A. Leeke, J. Cai, M. Jenkins, Solubility of Supercritical Carbon Dioxide in

Polycaprolactone (CAPA 6800) at 313 and 333 K, J. Chem. Eng. Data. 51 (2006) 1877–1879. https://doi.org/10.1021/je060230e.

[58] S. Areerat, E. Funami, Y. Hayata, D. Nakagawa, M. Ohshima, Measurement and prediction of diffusion coefficients of supercritical CO2 in molten polymers, Polym. Eng. Sci. 44 (2004) 1915–1924. https://doi.org/10.1002/pen.20194.

[59] H. Eslami, F. Müller-Plathe, Molecular Dynamics Simulation of Sorption of Gases in Polystyrene, Macromolecules. 40 (2007) 6413–6421. https://doi.org/10.1021/ma070697+.

[60] C.O. Dinç, A. Güner, Solubility profiles of poly(ethylene glycol)/solvent systems, I: Qualitative comparison of solubility parameter approaches, Eur. Polym. J. 43 (2007) 3068–3093. https://doi.org/10.1016/j.eurpolymj.2007.02.022.